Virology 526 (2019) 117–124

Contents lists available at ScienceDirect

Virology

journal homepage: www.elsevier.com/locate/virology

Physical interaction of RTBV ORFI with D1 protein of *Oryza sativa* and Fe/Zn homeostasis play a key role in symptoms development during rice tungro disease to facilitate the insect mediated virus transmission

P. Srilatha[a], Faisal Yousuf[b], Ramesh Methre[b], T. Vishnukiran[b], Surekha Agarwal[b], Yugandhar Poli[b], M. Raghurami Reddy[b], B. Vidyasagar[a], Chitra Shanker[b], D. Krishnaveni[b], S. Triveni[a], Brajendra[b], Shelly Praveen[c], S.M. Balachandran[b], D. Subrahmanyam[b], Satendra K. Mangrauthia[b,*]

[a] Professor Jayashankar Telangana State Agricultural University, Hyderabad 500030, India
[b] ICAR-Indian Institute of Rice Research, Hyderabad 500030, India
[c] ICAR-Indian Agricultural Research Institute, New Delhi 110012, India

ARTICLE INFO

Keywords:
Photosynthesis
Photosystem II
psbA
RTSV
Transmission
Green leafhopper

ABSTRACT

Rice tungro disease is caused by the combined action of Rice tungro bacilliform virus (RTBV) and Rice tungro spherical virus (RTSV). The RTBV is involved in the development of symptoms while RTSV is essential for virus transmission. We attempted to study the mode of action of RTBV in the development of symptoms. The tungro disease symptoms were attributed to viral interference in chlorophyll and carotenoids biosynthesis, photosynthesis machinery, iron/zinc homeostasis, and the genes encoding the enzymes associated with these biological processes of rice. The adverse effects of virus infection in photosystem II (PSII) activity was demonstrated by analyzing the Fv/Fm ratio, expression of *psbA* and *cab1R* genes, and direct interaction of RTBV ORF I protein with the D1 protein of rice. Since ORF I function is not yet known in the RTBV life cycle, this is the first report showing its involvement in regulating host photosynthesis process and symptoms development.

1. Introduction

Rice (*Oryza sativa*) is one of the most important staple food crops and plays a critical role in feeding more than half of the world population. It is also a model cereal crop to understand the molecular and physiological mechanisms of biological processes and stress tolerance. The crop is host for numerous fungal, bacterial and viral pathogens which are major factors responsible for reducing the production and productivity of rice. The tungro disease of rice is a most important viral disease prevalent in South and South East Asia (Azzam and Chancellor, 2002). In India, the virus caused epidemics during the years 1984, 1988, 1990 and 2001 (Muralidharan et al., 2003).

Tungro is a complex disease caused by a combination of two different viruses, i.e., RTBV (Rice tungro bacilliform virus), a double-stranded circular DNA virus, belonging to family caulimoviridae and RTSV (Rice tungro spherical virus), a linear single-stranded RNA virus, belonging to family Sequiviridae (Sailaja et al., 2013; Hull, 1996; Mangrauthia et al., 2012). The disease exhibits symptoms such as stunting, yellow to yellow-orange leaf discoloration, twisting of leaf tips and reduced ear-bearing tillers in rice (Hull, 1996; Azzam and Chancellor, 2002; Singh et al., 2015). RTBV is considered as the primary causal agent for development of disease symptoms while RTSV facilitates the transmission of the disease by the insect vector green leafhopper (GLH, *Nephotettix virescenes*, and *N. nigropictus* Stal) in a semi-persistent manner (Hibino et al., 1978; Azzam and Chancellor, 2002). RTSV is transmitted independently while RTBV requires RTSV or RTSV-related helper factor for the transmission by GLH. So far, no other means of virus transmission has been reported in the case of rice tungro disease.

Many efforts have been made to understand the genomes and genes of tungro disease-causing viruses (Hull, 1996; Jones, 1991; Marmey et al., 2005; Mathur and Dasgupta, 2007; Rajeswaran et al., 2014), however, only a few studies have been attempted to investigate the physiological or molecular basis of host-virus interaction (Dai et al., 2008; Mangrauthia et al. 2017a; Singh et al., 2015). There is need to understand the physiological and biochemical changes induced by

* Corresponding author.
E-mail address: Satendra.KM@icar.gov.in (S.K. Mangrauthia).

https://doi.org/10.1016/j.virol.2018.10.012
Received 9 July 2018; Received in revised form 10 October 2018; Accepted 11 October 2018
Available online 26 October 2018
0042-6822/

tungro disease in rice and to establish their correlation with symptoms development and vector interaction. Such studies are crucial to develop effective virus management strategies in rice. Despite extensive efforts made to develop tungro disease resistance in rice through breeding or transgenic approaches, success could not be achieved in terms of the development of commercialized virus resistant rice varieties (Lee et al., 2010; Shim et al., 2015; Tyagi et al., 2008).

In this study, we analyzed the effect of tungro disease in photosynthesis, chlorophyll biosynthesis, and Fe/Zn homeostasis of rice. The expression of genes encoding chlorophyll biosynthesis enzymes, photosynthetic components, and enzymes associated with Fe and Zn metabolism was determined to substantiate the physiological observations. The impact of yellowing symptoms on insect vector orientation was also studied.

2. Material and methods

2.1. Plant material and virus isolates

The rice cultivar Taichung Native 1 (TN1) was used in this study. The Hyderabad isolate of the RTBV and RTSV were used for the virus inoculation and disease development.

2.2. Inoculation of the virus and confirmation

The virus was inoculated into 15 days old TN1 plants grown in plastic pots in the glass house. Insect vector-mediated inoculation of the virus was done by tube method (Cabauatan et al., 1995). Insects (GLH) were released on infected plants for 24 h to acquire the virus and transferred to healthy plants for 6 h for inoculation @3 viruliferous insects per plant. The disease symptoms on infected plant leaves were observed after 15–20 days of inoculation. To confirm the presence of RTBV and RTSV in infected plants, PCR (polymerase chain reaction) and RT- PCR (reverse transcription-PCR) were done using virus gene-specific primers as reported in our previous studies (Malathi and Mangrauthia, 2013; Mangrauthia et al., 2010).

2.3. Chlorophyll and carotenoids estimation

Four biological replicates of diseased and healthy (hereafter 'control') plants were used for measurement of chlorophyll-a, chlorophyll-b, total chlorophyll and carotenoids in 45 days old plants. Leaf chlorophyll pigments were extracted by using 80% cold acetone. Chlorophyll and carotenoids were determined by spectrophotometer-spectroscan UV 2600 (Toshniwal Instruments Pvt. Ltd., India). Leaf chlorophyll pigments were estimated by the method described by Lichtenthaler and Wellburn (1983).

2.4. Photosynthetic parameters and chlorophyll fluorescence

Photosynthetic parameters such as net photosynthetic rate (P_N), stomatal conductance (g_s),transpiration rate (E), and intercellular CO_2 concentration (C_i) were recorded in 45 days old plants by using Li-Cor 6400 (IRGA) portable photosynthesis measurement system attached to leaf chamber fluorometer (LCF Model 6400-1, LICOR, USA) which was used as artificial light source. During measurements, the PAR (Photosynthetically Active Radiation) was kept at 1200 μmol m^{-2} s^{-1}. The CO_2 concentration was kept at 387 ± 6 ppm. Chlorophyll fluorescence was measured with a portable PAM-210 fluorometer (Walz, Effeltrich, Germany). Various fluorescence parameters like maximum efficiency of open PS II reaction centers, electron transport rate, the quantum yield of PS II photochemistry, and non-photochemical quenching were estimated in dark adapted leaves. Four biological replicates of control and diseased plants were used for these experiments.

2.5. Primer designing

Real-Time PCR primers for ten genes associated with chlorophyll metabolism and photosynthesis process were synthesized based on an earlier study (Wu et al., 2007). These genes are Glutamyl t- RNA reductase (*HEMA1*), NADPH: Pchlideoxidoreductase (*PORA*), Chlorophyllide A oxygenase 1 (*CAO1*), Chlorophyll a-b binding protein 1(*cab1R*), Chlorophyll a-b binding protein 2(*cab2R*), Photosystem I P700 apoprotein A (*psaA*), Photosystem II - D1 protein (*psbA*), Rubisco larger subunit (*rbcL*), Rubisco smaller subunit (*rbcS*), and Yellow green leaf 1(*ygl1*). Eleven other genes (*NAS1, NAS2, NAS3, IRT1, IRT2, ZIP4, ZIP8, YSL1, YSL15, NRAMP1,* and *DMAS1*) associated with iron and zinc homeostasis in rice were used for quantitative expression analysis. Primer details of these genes are described in our earlier report (Agarwal et al., 2014).

2.6. RNA isolation, cDNA preparation, and quantitative real time PCR

Total RNA was isolated from three replicates of control and diseased plants by RNeasy Plant Mini Kit (Qiagen) following the manufacturer's protocol. cDNA was prepared by using the ImProm-II™ Reverse Transcription System (Promega) with oligo dT primers. cDNA was treated with RNase H and normalized to equal concentration for real-time PCR experiments. Quantitative real-time PCR (RT-qPCR) was performed by using SYBR Premix Ex-Taq kit (Takara). Actin was chosen as an internal control and all the reactions were run in triplicate. Amplification conditions maintained were 50 °C for 10 min for the pre-holding stage, 95 °C for 10 min for holding stage, 40 cycles of denaturing at 95 °C for 15 s and annealing/ extension at 60 °C for 30 s, followed by a disassociation stage (melting curve analysis). Reactions were performed in Light Cycler 96 Real-Time PCR System (Roche).

2.7. Analysis of RT-qPCR data

Analysis of the gene expression data was done using the $2^{-\Delta\Delta Ct}$ method (Livak and Schmittgen, 2001). C_T (threshold cycle) value of the target gene was normalized with C_T of the respective reference gene and expressed as ΔC_T (Target/Reference ratio). ΔC_T values of the diseased sample were further normalized with the ΔC_T value of the control to obtain the $\Delta\Delta C_T$ value ($\Delta\Delta C_T$ = ΔC_T (diseased) - ΔC_T (control). The fold change in gene expression was calculated by $2^{-\Delta\Delta CT}$. The standard deviation and fold change expression were calculated as described in our previous study (Mangrauthia et al. 2017b).

2.8. Yeast two-hybrid assay

Coding DNA sequences of RTBV ORFs, i.e. ORFI, ORF II and ORF IV whose functions are not very well understood, were cloned into pGADT7 and pGBKT7 vectors. Also, a rice gene *psbA* (NCBI: JN861110) encoding the D1 protein that plays important role in PSII activity, was cloned into pGADT7 and pGBKT7 vectors. The interaction of all the three viral proteins was tested with rice protein. Yeast two-hybrid (Y2H) assays were done using the Matchmaker Gold Yeast Two-Hybrid System (Clontech). The protocol described in the kit was followed for Y2H assay. The yeast growth media (YPD medium, Clontech), SD growth medium w/o amino acids (Himedia) and supplements media (Clontech) were used for the Y2H experiment.

2.9. Atomic absorption spectrophotometer (AAS) analysis

Iron and zinc content in soil samples of the rhizosphere of control and diseased plants were estimated by AAS (Varian AA- 240 at. Absorption Spectrophotometer). Ten grams of air-dried soil sample was put into 150 ml conical flask. 20 ml of the DTPA (Diethylene triamine penta acetic acid) was added and then closed by the polythene stoppers. The soil samples were shaken for 2 h on a horizontal shaker. After

shaking, the extract was filtered through Whatman No.42 filter paper for estimation of iron and zinc content by AAS (absorbance at 213.86 nm for zinc and 248.33 nm for iron).

To analyze the iron and zinc content in the leaves of control and diseased plant samples, one gram of the powdered leaf sample was put into a 100 ml micro-Kjeldahl flask. 5 ml of the concentrated tri-acid mixture (9:5:1 of HNO_3:H_2SO_4: $HClO_4$) was added and kept for digestion for 2 h. When it turned into a clear transparent solution, 20 ml of deionized or distilled water was added and filtered through Whatman No.1 filter paper. The diluted digest was transferred into the 50 ml volumetric flask, and the final volume was made to 20 ml with deionized water. Aliquots of this diluted digest were used for the determination of iron and zinc by AAS.

2.10. Quantification of the RTBV and RTSV in TN1 plants grown in iron, zinc, and magnesium differential media

Seeds were kept for germination in Petri plates and allowed to grow for 12 days. After 12 days, roots of seedlings were thoroughly washed with distilled water and then transferred to dark-colored plastic glasses containing differential nutrient media prepared from Hoagland solutions. Stock solutions were used to prepare the differential media. The details of nutrient media used in this study are given in Table S1. Fifteen days old seedlings were inoculated with the virus using GLH. Leaf samples were collected from 30 days old virus inoculated plants for DNA and RNA extraction. DNA was extracted using the CTAB method (Murray and Thompson, 1980) while RNA was isolated by RNeasy Plant Mini Kit (Qiagen). The isolated DNA was treated with RNase A and normalized to equal concentration for quantification of RTBV using SYBR Premix Ex-Taq kit (Takara), as reported previously (Malathi and Mangrauthia, 2013). The RNA was converted to cDNA using ImProm-II™ Reverse Transcription System (Promega) with oligo dT primers. The cDNA was treated with RNase and normalized to equal concentration. The forward primer- 5′ CAA GAG CCA ATT TGC TCA TGA TG 3′ and reverse primer- 5′ GCA TAC TTG AAG GCT CGT TTC TT 3′ were used for quantification of RTSV using cDNA and SYBR Premix Ex-Taq (Takara) kit. All the reactions of RT-qPCR were run in triplicate. The mean Ct was used for calculating the relative expression and comparing the RTBV and RTSV population in plants grown in normal (control) and differential nutrient media.

2.11. Orientation of the insect vectors

2.11.1. Visual cues

To observe the preference of insects (GLH) towards diseased or healthy plants through visual sense, the pots were kept in a cage having the same age and density of the TN1 plants. In the center of the two pots, one Petri plate with 50 no. of 24 h starved GLH insects was placed (Fig. S1). After 2 h, the number of GLH was counted separately on the diseased and healthy plants. The experiment was done in four independent replications.

2.11.2. Olfactory cues

The six arm olfactometer was used to determine the orientation of the insects towards the volatiles of healthy and diseased leaves (Fig. S1). The olfactometer consists of a central chamber with six glass tubes of 20 cm length and 2.5 cm diameter projected outwards at equidistance. Air was blown into the central cell, arms and odour cells to remove any odour in the olfactometer. Insects were kept in BOD (Biochemical Oxygen Demand) incubator at 23 ± 2 °C for 1 h before placing them in the olfactometer. At the center of the olfactometer, 50 insects were released. Diseased and healthy leaves were placed in 6 glass tubes alternatively. Similarly, leaf extract was also used to study the insect orientation. Here, 1 mg of the leaf was extracted with 1 ml methanol and incubated overnight at room temperature. The extract was centrifuged at 13,000 rpm for 5 min. The supernatant was transferred into a fresh Eppendorf tube. 30 µl of the supernatant obtained from healthy and diseased leaf was placed individually in blotting paper strip. 30 µl methanol was used as a control. These 3 strips were placed in olfactometer arms alternatively.

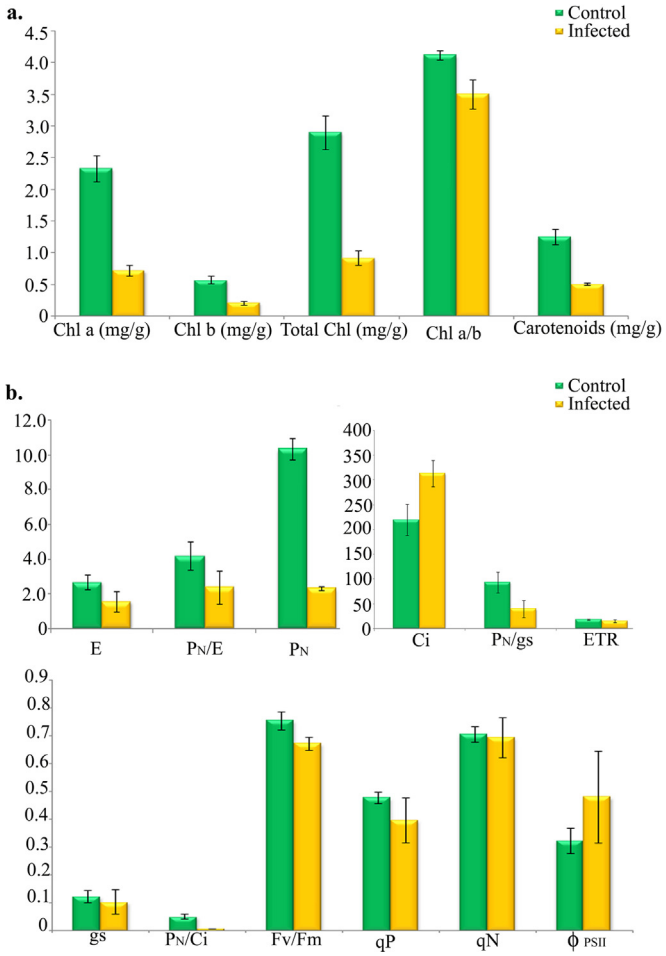

Fig. 1. (a) Analysis of chlorophyll-a, chlorophyll-b, total chlorophyll, and carotenoids in control and virus infected TN1 plants. Y axis- the mean value obtained from four biological replicates. (b) Photosynthetic parameters of control and virus infected TN1 plants. E- transpiration rate (mmol(H_2O) m^2s^{-1}), P_N-net photosynthetic rate (µmol(CO_2)m^{-2} s^{-1}), Ci- intercellular CO_2 concentration (ppm), gs- stomatal conductance (mol m^{-2} s^{-1}), ETR-electron transport rate, Fv/Fm-maximal quantum yield of PSII, qP- photochemical quenching, qN- non-photochemical quenching, ΦPSII-photochemical yield of photosystem II. Y axis-the mean value obtained from four biological replicates.

3. Results

3.1. Tungro disease causes the reduction in chlorophyll and carotenoids content

The chlorophyll and carotenoids content was examined in control and virus-infected plants. The mean value of chlorophyll-a was 2.33 ± 0.21 mg/g and 0.72 ± 0.09 mg/g in control and infected plants, respectively. Similarly, chlorophyll-b was 0.57 ± 0.06 mg/g and 0.21 ± 0.03 mg/g in control and infected plants, respectively. The total chlorophyll was 2.90 ± 0.27 mg/g in control plants and 0.92 ± 0.11 mg/g in infected plants. The carotenoids content was1.25 ± 0.12 mg/g and 0.51 ± 0.02 mg/g in control and infected plants, respectively. Overall, the chlorophyll and carotenoids content was reduced significantly in tungro disease affected plants as compared to control plants (Fig. 1a).

3.2. Tungro disease affects photosynthesis

In order to study the effects of the tungro disease in the photosynthesis of rice, various parameters were studied in four different replications. The net photosynthetic rate was 10.360 ± 0.628 and 2.317 ± 0.102 in control and infected plants, respectively. Similarly, transpiration rate was also reduced in infected plants as compared to control. The mean value of transpiration rate was 2.686 ± 0.405 in control plants and 1.567 ± 0.567 in infected plants. Interestingly, the intercellular CO_2 concentration was increased in the infected plants. The mean value of intercellular CO_2 was 219.847 ± 32.008 ppm and 313.544 ± 26.278 ppm in control and infected plants, respectively. The mean Fv/Fm ratio, representing the efficiency of the PSII, was significantly reduced (17%) in infected leaf compared to control leaf. Whereas, other parameters like apparent electron transport rate (ETR), photochemical quenching (qP), non-photochemical quenching (qN), and photochemical quantum yield (Φ_{PSII}) did not show the statistically significant difference (Fig. 1b).

3.3. Photosynthesis and chlorophyll metabolism related genes are differentially regulated during tungro disease

Gene expression analysis was carried out in control and virus-infected plants. Ten genes encoding enzymes involved in chlorophyll metabolism and photosynthesis were analyzed for their expression. In comparison to control, virus infected plants showed upregulation of *HEMA1, PORA, COA1*, and *cab2R* and down-regulation of *cab1R, psaA, psbA, rbcL, rbcS*, and *ygl1* genes. Maximum upregulation of 12.539 fold was recorded for *PORA* gene while maximum down-regulation of −17.09 and −24.1 fold was recorded in case of *psaA* and *psbA,* respectively. Overall, the gene expression analysis suggested that the chlorophyll and photosynthesis-associated genes are significantly affected during the virus infection in rice (Fig. 2 a).

3.4. RTBV-ORF I interacts with Oryza sativa D1 protein

To decipher if the reduction in PSII efficiency of rice during tungro disease is due to direct interaction of viral proteins with host proteins, we performed the Y2H assay. The protein-protein interaction study showed that rice D1 protein directly interacts with RTBV-ORF I. D1 protein encoded by *psbA* gene was selected for Y2H assay because it showed maximum change in expression (-24.1 fold) after virus infection. The reduced Fv/Fm (representing the efficiency of the PSII) and down regulation of *cab 1R* (light-harvesting chlorophyll a/b binding proteins) indicated that PSII is severely affected during tungro disease. The D1 protein binds the essential redox components of PSII required for primary charge separation and subsequent electron transfer. Yeast cells expressing binding domain (BD)-*psbA* and activation domain (AD)-ORF I grew on both minus-three media (media without amino acids-leucine, tryptophan, and histidine) and minus-four media (media without leucine, tryptophan, histidine, and adenine), suggesting a strong protein-protein interaction between ORF I and D1 protein. The other two ORFs of RTBV (ORF II and ORF IV) did not show any interaction with the D1 protein (Fig. 2 b).

3.5. Tungro disease affects iron and zinc homeostasis in rice

Considering the central role of Fe in chlorophyll biosynthesis and the key role of Zn and Fe in catalysis of important enzymes involved in DNA replication, transcription and other essential biological processes, estimation of these two elements was done in control and virus-infected leaf samples. The Fe content was 3.056 ppm and 2.424 ppm in control and virus-infected plant leaves, respectively. Similarly, Zn content was 0.148 ppm and 0.109 ppm in control and virus-infected plant leaves, respectively. Also, the soil samples were analyzed from the rhizosphere of control and virus-infected plants. Fe and Zn content of soil samples showed no significant difference (Fig. 3a).

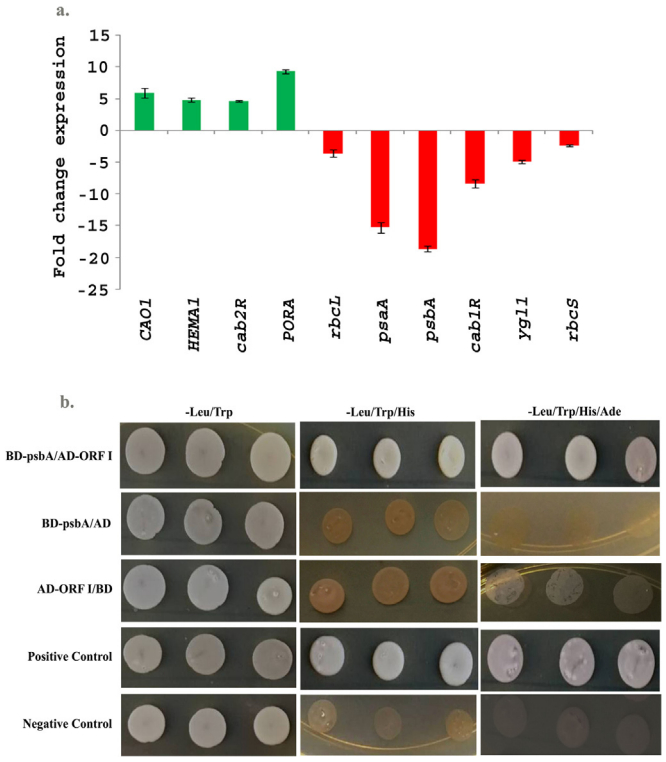

Fig. 2. (a) Expression analysis of genes associated with photosynthesis and chlorophyll metabolism through RT-qPCR. The fold change expression of genes in infected plants was calculated by comparing their expression in control plants. Y-axis shows the fold change expression of genes. Bars represent the mean ± S.E. of three biological replicates. Green color bars indicate upregulation and red color as down-regulation. (b) Tests of RTBV ORFI and *O. sativa* psbA interaction by yeast two-hybrid assays. Full-length protein of psbA (D1) was fused with the GAL4 binding domain (BD). Full-length ORFI was fused with GAL4 activation domain (AD).

3.6. Fe and Zn homeostasis related genes are differentially regulated during tungro disease

To analyze the expression of genes associated with Fe and Zn metabolism of rice, eleven genes were selected based on their crucial functions reported in our earlier study (Agarwal et al., 2014). Interestingly, most of the genes showed down-regulation in virus-infected rice samples except *NRAMP1* and *NAS2* which were up-regulated by 17.46742 and 4.162614 fold, respectively. The considerable down-regulation was noticed in expression of genes such as *NAS1, IRT2, ZIP8, YSL1, YSL15, NAS3, ZIP4, IRT1* and *DMAS1* which showed −17.23, −3.715, −0.20268, −12.935, −8.775, −16.09, −42.435, −16.315 and −5.225 fold change expression, respectively. Expression analysis of eleven genes revealed that virus infection alters the regulation of genes encoding enzymes or proteins associated with Fe and Zn homeostasis in rice (Fig. 3 b).

3.7. Accumulation of RTBV in rice is reduced in the presence of high Fe and Zn in growth medium

To further understand the role of Fe and Zn in RTBV and RTSV multiplication, TN1 plants were grown in six different Hoagland medium, i.e. Fe deficient, 2X Fe, Zn deficient, 2X Zn, Mg deficient, 2X Mg, and a normal solution with the recommended concentration of all the nutrients. Real-time PCR was used to measure the relative population of RTBV and RTSV in plants grown in these nutrients media. The

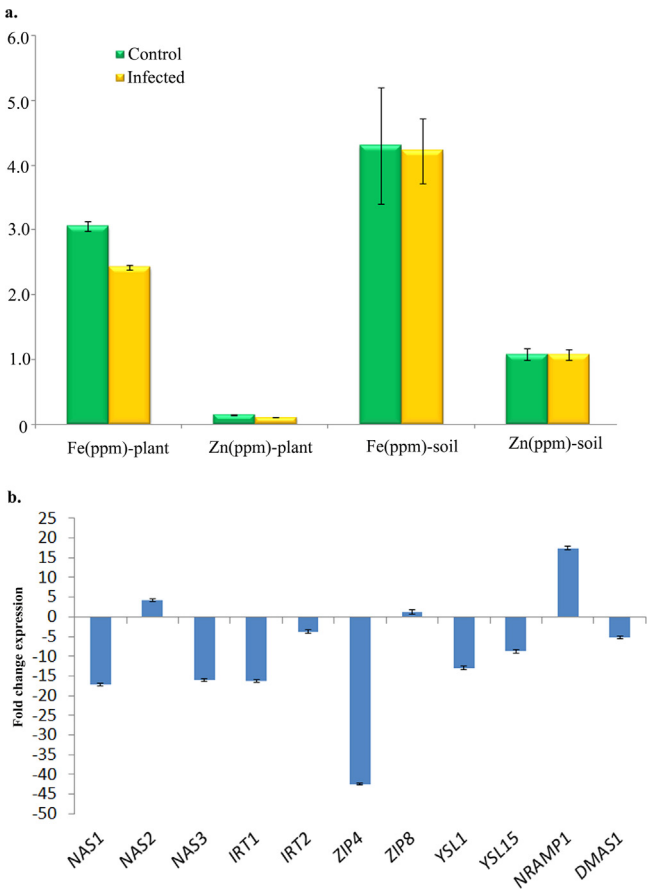

Fig. 3. (a) Analysis of iron (Fe) and Zinc (Zn) content in control and virus infected TN1 plants and their rhizosphere soil. Y axis- the mean value obtained from four biological replicates. (b) Expression analysis of genes associated with Fe and Zn homeostasis in rice through RT-qPCR. The fold change expression of genes in infected plants was calculated by comparing their expression in control plants. Y-axis shows the fold change expression of genes. Bars represent the mean ± S.E. of three biological replicates.

Fe, Zn, and Mg showed considerable effects on accumulation of RTBV and RTSV. Interestingly, the RTBV was drastically reduced in 2X media of Fe and Zn (Fig. 4).

3.8. Green leafhoppers are more attracted to virus-infected plants through visual cues

The insect vector's orientation was studied through two different experiments, i.e., visual cues and olfactory cues. The mean number of insect vectors attracted to the infected plants with yellow leaves was higher than those attracted to healthy plants with green leaves through visual cues. In the case of olfactory cues, a significant difference was not observed in the number of insects attracted to control and diseased plants (Fig. 5).

4. Discussion

Tungro disease is one of the most important viral diseases known for its devastating effects on rice cultivation in South and South-East Asia (Azzam and Chancellor, 2002; Muralidharan et al., 2003). The characteristic symptoms of the tungro disease are yellowing of leaves and stunting. This study was attempted to understand the physiological and molecular processes responsible for causing these symptoms. Also, the symptomatic manifestations were correlated with the preferential feeding of GLH in virus-infected plants which in turn facilitates the transmission of the virus.

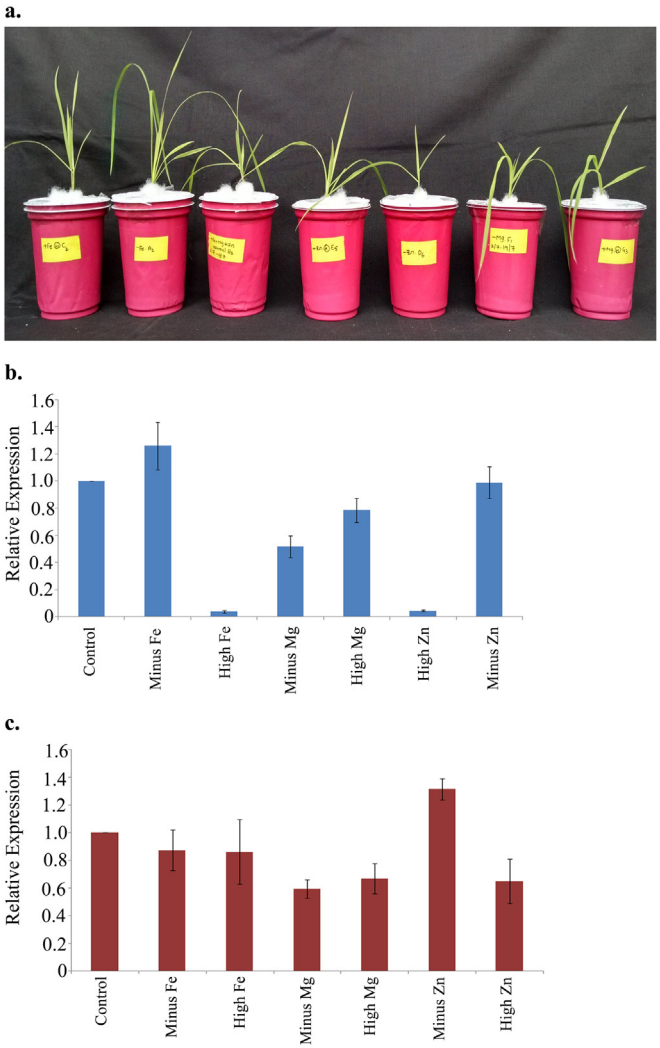

Fig. 4. (a) Rice cv. TN1 plants growing in differential media of Fe, Zn and Mg (b) Quantification of RTBV using RT-qPCR (c) Quantification of RTSV using RT-qPCR. The bars on Y-axis represent the relative expression.

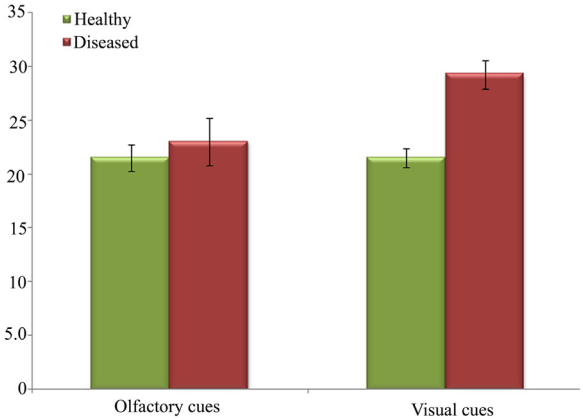

Fig. 5. Analysis of insect vector orientation to control (healthy) and virus infected (diseased) TN1 plants through olfactory and visual cues. Y axis- the mean number of insects obtained from four biological replicates.

Significant reduction in Chlorophyll a & b, total chlorophyll, and carotenoids was observed in virus-infected TN1 plants. Decreased level of chlorophyll content due to tungro disease was reported earlier also (Jabeen et al., 2017; Sridhar et al., 1978). The reduction in Chl a was

more pronounced than Chl b which was in concurrence with the earlier reports (Yadav and Mishra, 1987; Subbarao et al., 1979). The net photosynthetic rate and transpiration rate were reduced significantly in virus-infected plants. The reduction in photosynthetic activity and transpiration rate due to tungro disease was reported in earlier studies (Mohanty et al., 1979; Singh et al., 1990). Interestingly, this study shows an increase in intercellular CO_2 concentration in tungro disease affected rice plants. This is the first report showing the detailed analysis of P_N, g_s, E and C_i on control and virus-infected rice plants.

The tungro disease caused upregulation of four photosynthesis-related genes, i.e. *HEMA1*, *PORA*, *CAO1*, and *cab2R*. *HEMA1* encodes a key enzyme involved in the tetrapyrrole synthesis during chlorophyll biosynthesis. The reduced chlorophyll during tungro disease might be inducing *HEMA1* for more synthesis of tetrapyrrole to compensate the chlorophyll loss. Very high upregulation (12.53 fold) of PORA, a negatively regulated enzyme involved in the light-induced greening of higher plants (Masuda et al., 2003), might be one probable factor for yellowing of the leaves during tungro disease. Chlorophyllide a oxygenase (CAO) catalyzes the last step of chlorophyll biosynthesis by converting Chl a to Chl b. Among the two homologous *CAO* genes, *OsCAO1* has a primary role and encodes the only enzyme responsible for Chl b synthesis and chloroplast development during the light in rice (Yang et al., 2016). The upregulation of *OsCAO1* might be responsible for the more severe reduction in Chl a as compared to Chl b during the tungro disease. Notably, Chl a/b ratio was reduced from 4.12 in control plants to 3.51 in virus-infected plants. Increased expression of CAO resulted in increased Chl b levels (Biswal et al., 2012). The light-harvesting chlorophyll a/b binding proteins (cab) play a positive role in guard cell signaling in response to ABA (Xu et al., 2012). The reduced transpiration rate observed during tungro disease might be due to the altered expression of cab genes. Interestingly, our study showed upregulation of *cab2R* and down-regulation of *cab1R* during tungro disease. Using the ygl1 mutant, Wu et al. (2007) showed that both of these genes are differentially regulated. Among the genes we examined, all the upregulated genes (*HEMA1, PORA*, *CAO1*, and *cab2R*) are nucleus-encoded genes.

Six genes – *cab1R, psaA, psbA, rbcl, rbcs,* and *ygl1* showed down-regulation. Among the down-regulated genes, *psaA, psbA,* and *rbcL* are plastid-coded genes while *cab1R, rbcS,* and *ygl1* are nucleus-encoded genes. Rubisco, the most abundant protein in plants, catalyzes the first steps in CO_2 fixation during photosynthesis (Lorimer, 1981). The synthesis of the Rubisco holoenzyme requires the coordinated expression of genes from both nucleus (encoding eight small subunits-RBCS) and plastid (encoding eight large subunits-rbcL) (Suzuki and Makino, 2012). The down-regulation of both *rbcL* and *rbcS* during tungro disease provided another evidence of coordinated expression of these genes. The decreased expression of *rbcL* and *rbcS* may be primarily responsible for the increased intercellular CO_2 during tungro disease. Many fold down-regulation of the plastid genes *psaA* (encoding the P700 apoproteins of photosystem I) and *psbA* (encoding the D1 protein of photosystem II) (Hiratsuka et al., 1989) and reduction in Fv/Fm suggests that both the photosystems are affected due to the virus infection in rice. The Y2H assay showed that ORFI protein of RTBV directly interacts with the D1 protein of rice. Our results suggest that the decreased expression of the *psbA* gene and reduction in PSII efficiency might be due to direct interaction of RTBV ORFI with D1 protein followed by feedback inhibition of *psbA* gene expression. Notably, the function of RTBV ORFI is not known. This study revealed that ORFI plays an important role in host-virus interaction by regulating photosynthesis machinery of rice and contributing to symptoms development. In an interesting study, Kong et al. (2014) showed that disease-specific protein (SP) of Rice stripe virus (RSV) interact with PsbP protein (an oxygen-evolving complex protein) of rice which plays a key role in RSV disease symptoms development.

Expression of the *ygl1* and *cab1R* was also reduced due to virus infection. The *ygl1* encodes chlorophyll synthase and the mutation of this gene displayed yellow-green leaves in young rice plants. The ygl1 mutants showed decreased Chl synthesis, increased level of tetrapyrrole intermediates, delayed chloroplast development, and severe reduction of the *cab1R* transcript (Wu et al., 2007). The down-regulation of *ygl1* and *cab1R* during tungro disease suggests that these genes might be functioning in coordination during chlorophyll biosynthesis or chloroplast development. Down-regulation of *cab 1R* provides further evidence that PSII efficiency is severely affected during tungro disease. HEMA1 encodes enzyme involved in tetrapyrrole biosynthesis while ygl1 mutation shows the increased level of tetrapyrrole intermediates (Wu et al., 2007), suggesting that the expression of these genes may be antagonistic. Interestingly, we observed the down-regulation of *ygl1* and up-regulation of *HEMA1* during tungro disease in rice.

Out of the 11 genes involved in Fe and Zn homeostasis, 9 genes showed down-regulation while 2 genes, i.e. *OsNRAMP 1* and *OsNAS2* were upregulated during the tungro disease in rice. The genes encoding natural resistance-associated macrophage proteins (NRAMPs) have been demonstrated to be involved in Fe uptake and transport function (Wei et al., 2009; Curie et al., 2000). Nicotianamine synthase (NAS) catalyzes the first step in the biosynthesis of mugineic acid family phytosiderophores (MAs) that solubilize Fe and plays a key role in the long-distance transport of Fe (Takagi, 1976). Three rice NA synthase (NAS) genes- *OsNAS1, OsNAS2*, and *OsNAS3* are differentially regulated by Fe (Inoue et al., 2003). Tungro disease resulted in increased expression of *NAS2* and decreased expression of *NAS1* and *NAS3*. Expression of *OsNAS3* was suppressed by Fe deficiency (Inoue et al., 2003). The reduced expression of *OsNAS3* in virus-infected plants might be due to Fe deficiency in the leaves. It should be noted that Fe was reduced from 3.056 ppm in the control plant to 2.424 ppm in virus-infected plants. Another gene *OsDMAS1* involved in MA biosynthesis (Bashir et al., 2010) was also down-regulated.

Fe transport-related genes such as Fe-regulated transporters (*OsIRT1* and *OsIRT2*) (Bughio, 2002; Ishimaru et al., 2006), and Yellow stripe like (YSL) family of proteins (YSL1 and YSL15) (Koike et al., 2004) were down-regulated during tungro disease. The Zinc-Regulated Transporter, Iron-Regulated Transporter (ZRT-IRT)-like proteins (ZIPs) are vital metal transporters associated with transport of Zn in rice (Ishimaru et al., 2006; Takahashi et al., 2011). In this study, ZIP4 and ZIP 8 showed down-regulation due to virus infection in rice. It should be noted that Zn was reduced from 0.148 ppm in the control plant to 0.109 ppm in virus-infected plants. Overall, reduced level Fe and Zn content in tungro disease affected leaves and down-regulation of most of the genes associated with the uptake and transport of these nutrients suggest that the virus severely affects the Fe and Zn homeostasis in rice. In plants, Fe is crucial for the synthesis of chlorophyll and is a key component involved in the maintenance of structure and function of the chloroplast. Both Fe and Zn are essential components of many vital enzymes involved in photosynthesis, electron transport, DNA replication, transcription and protein synthesis etc. thus required for most of the biological functions (Rout and Sahoo, 2015). The relative quantification of RTBV and RTSV in nutrients differential media suggested that Fe and Zn have a significant impact on RTBV and RTSV multiplication. The RTBV population was very much reduced in 2X media of Fe and Zn.

In order to understand if the yellowing symptoms caused by the virus through interference in photosynthetic machinery and Fe/Zn homeostasis, is the deliberate strategy adapted by the virus to facilitate its transmission by green leafhopper, vector orientation was studied through visual and olfactory cues. Interestingly, we did not observe any difference in GLH orientation to diseased or healthy plants through olfactory cues. However, more GLH showed attraction to diseased yellow leaves as compared to healthy green leaves through visual cues. This study suggests that yellow symptoms caused by tungro disease might be required for the virus to facilitate its transmission by attracting more number of insect vectors. Various studies have reported that virus infection can alter olfactory and visual cues of infected plants

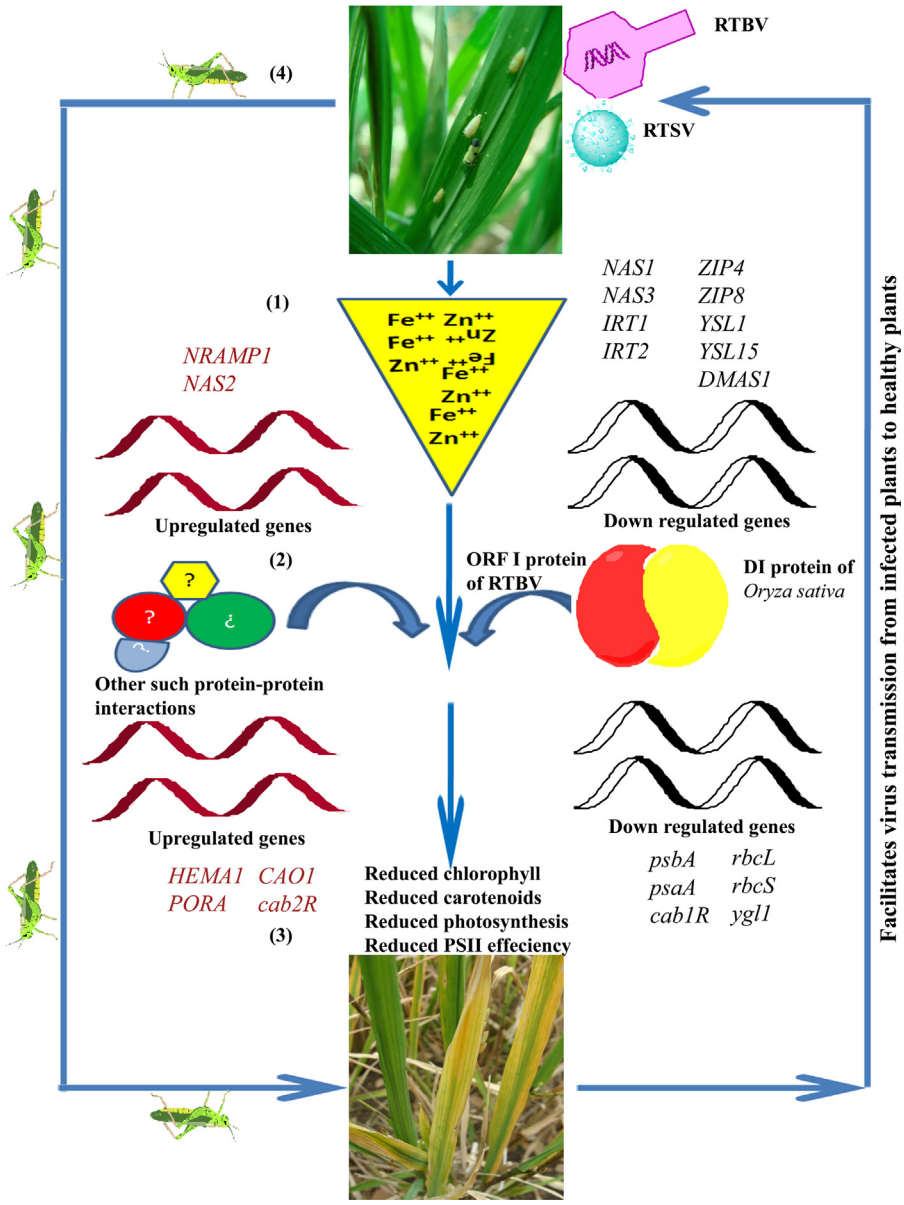

Fig. 6. A working model of the symptoms development process in rice during tungro disease and its implication in virus transmission through green leafhopper. (1) Infection of rice plant by RTBV and RTSV reduces Fe and Zn concentration in infected leaves. Several key genes involved in homeostasis of Fe and Zn get down-regulated in virus-infected tissue. (2) RTBV ORF I binds to D1 protein (encoded by *psbA*) of rice and reduces its transcription through feedback inhibition. Several other important genes of the photosynthesis process get down-regulated. (3) The perturbed Fe/Zn homeostasis and photosynthesis machinery (genes and proteins) of rice results in the reduction of chlorophyll, carotenoids, photosynthesis and photosystem II efficiency. Due to this, plants exhibit yellowing in leaves and stunting. (4) Such plants attract more green leafhoppers. These insect vectors help in transmission of the virus from infected plants to healthy plants.

and subsequently bring changes in the ecological interactions among plants and insects (Srinivasan et al., 2006; McMenemy et al., 2012; Shapiro et al., 2012). The changes caused by virus infection may enhance host plant quality for insect vectors, and aid in their orientation, settling, and reproduction on infected plants, while others may decrease host quality, favoring rapid vector dispersal from infected plants (Mauck et al., 2012).

RTBV is primarily responsible for causing yellowing and other typical symptoms of the tungro disease, while RTSV is known for its role in virus transmission (Hull, 1996). This study suggests that RTBV might be causing yellowing of rice leaves by regulating the photosynthesis machinery through ORFI, and Fe/Zn homeostasis. It should be noted that the differential media of Fe and Zn showed a significant difference in the RTBV multiplication. Therefore, RTBV proteins might be inducing the symptoms through subverting the rice Fe and Zn homeostasis, chlorophyll biosynthesis, and photosynthesis process. These symptoms caused by tungro disease may be a deliberate strategy of the virus to attract the insect vectors for transmission of virus complex (Fig. 6). Regulation of host photosynthetic machinery by viral protein to facilitate its transmission brings a new dimension to understand the host-virus interaction and develop effective management strategies.

Acknowledgements

Authors are highly thankful to the Director, ICAR-Indian Institute of Rice Research, for his kind support. This study was financially supported by the Department of Biotechnology, Government of India (Grant No. BT/PR8648/AGR/36/784/2013). We are also grateful to anonymous reviewers for their constructive suggestions to improve this manuscript. Authors thank Ms. Bhavya for helping in Editing of manuscript.

Conflict of interest

The authors declare that they have no conflict of interest.

Authors contributions

Conceived and designed the experiments: SKM, and SP. Performed the experiments: PS, SKM, FY, RM, TV, SA, YP, RRM, CS, DK, BV, ST, and B. Contributed reagents/equipments/materials/analysis tools: SMB and DS. Wrote the article: SKM, SP, CS, and PS. All authors read and approved the final manuscript.

Appendix A. Supporting information

Supplementary data associated with this article can be found in the online version at doi:10.1016/j.virol.2018.10.012.

References

Agarwal, S., TVGN, Venkata, Kotla, A., Mangrauthia, S.K., Neelamraju, S., 2014. Expression patterns of QTL based and other candidate genes in Madhukar × Swarna RILs with contrasting levels of iron and zinc in unpolished rice grains. Gene 546, 430–436.

Azzam, O., Chancellor, T.C.B., 2002. The biology, epidemiology, and management of rice tungro disease in Asia. Plant Dis. 86, 88–100.

Bashir, K., Ishimaru, Y., Nishizawa, N.K., 2010. Iron uptake and loading into rice grains. Rice 3, 122–130.

Biswal, A.K., Pattanayak, G.K., Pandey, S.S., Leelavathi, S., Reddy, V.S., Govindjee, Tripathy, B.C., 2012. Light intensity-dependent modulation of chlorophyll b biosynthesis and photosynthesis by overexpression of chlorophyllide a oxygenase in tobacco. Plant Physiol. 159, 433–449.

Bughio, N., 2002. Cloning an iron-regulated metal transporter from rice. J. Exp. Bot. 53, 1677–1682.

Cabauatan, P.Q., Cabunagan, R.C., Koganezawa, H., 1995. Biological variants of rice tungro viruses in the Philippines. Phytopathology 85, 77–81.

Curie, C., Alonso, J.M., Lejean, M., Ecker, J.R., Briat, J.F., 2000. Involvement of NRAMP1 from Arabidopsis thaliana in iron transport. Biochem. J. 347, 749–755.

Dai, S., Wei, X., Alfonso, A.A., Pei, L., Duque, U.G., Zhang, Z., et al., 2008. Transgenic rice plants that overexpress transcription factors RF2a and RF2b are tolerant to rice tungro virus replication and disease. Proc. Natl. Acad. Sci. USA 105, 21012–21016.

Hibino, H., Roechan, M., Sudarisman, S., 1978. Association of two types of virus particles with penyakit habang (tungro disease) of rice in Indonesia. Phytopathology 68, 1412–1416.

Hiratsuka, J., Shimada, H., Whittier, R., et al., 1989. The complete sequence of the rice (Oryza sativa) chloroplast genome: intermolecular recombination between distinct tRNA genes accounts for a major plastid DNA inversion during the evolution of the cereals. Mol. Gen. Genet. 217, 185–194.

Hull, R., 1996. Molecular biology of rice Tungro viruses. Annu. Rev. Phytopathol. 34, 275–297.

Inoue, H., Higuchi, K., Takahashi, M., Nakanishi, H., Mori, S., Nishizawa, N.K., 2003. Three rice nicotianamine synthase genes, OsNAS1, OsNAS2, and OsNAS3 are expressed in cells involved in long-distance transport of iron and differentially regulated by iron. Plant J. 36, 366–381.

Ishimaru, Y., Suzuki, M., Tsukamoto, T., et al., 2006. Rice plants take up iron as an Fe3+-phytosiderophore and as Fe2+. Plant J. 45, 335–346.

Jabeen, A., Kiran, T.V., Subrahmanyam, D., Lakshmi, D.L., Bhagyanarayana, G., Krishnaveni, D., 2017. Variations in chlorophyll and carotenoid contents in tungro infected rice plants. J. Res. Dev. 5, 1–7.

Jones, M.C., Gough, K., Dasgupta, I., et al., 1991. Rice tungro disease is caused by an RNA and a DNA virus. J. Gen. Virol. 72, 757–761.

Koike, S., Inoue, H., Mizuno, D., Takahashi, M., Nakanishi, H., Mori, S., Nishizawa, N.K., 2004. OsYSL2 is a rice metal-nicotianamine transporter that is regulated by iron and expressed in the phloem. Plant J. 39, 415–424.

Kong, L., Wu, J., Lu, L., Xu, Y., Zhou, X., 2014. Interaction between rice stripe virus disease-specific protein and host PsbP enhances virus symptoms. Mol. Plant 7, 691–708.

Lee, J.H., Muhsin, M., Atienza, G.A., et al., 2010. Single nucleotide polymorphisms in a gene for translation initiation factor (eIF4G) of rice (Oryza sativa) associated with resistance to rice tungro spherical virus. Mol. Plant-Microbe Interact. 23, 29–38.

Lichtenthaler, H.K., Wellburn, A.R., 1983. Determinations of total carotenoids and chlorophylls a and b of leaf extracts in different solvents. Biochem. Soc. Trans. 11, 591–592.

Livak, K.J., Schmittgen, T.D., 2001. Analysis of relative gene expression data using real-time quantitative PCR and the $2^{-\Delta\Delta CT}$ method. Methods 25, 402–408.

Lorimer, G.H., 1981. The carboxylation and oxygenation of ribulose 1,5-bisphosphate: the primary events in photosynthesis and photorespiration. Annu. Rev. Plant Physiol. 32, 349–383.

Malathi, P., Mangrauthia, S.K., 2013. Deciphering the multiplication behaviour of Rice tungro bacilliform virus by absolute quantitation through real-time PCR. Arch. Phytopathol. Plant Prot. 46, 2366–2375.

Mangrauthia, S.K., Jha, M., Agarwal, S., Sailaja, B., Rajeswari, B., Krishnaveni, D., 2017b. Delineation of gene expression pattern in rice under Rice tungro virus and green leafhopper infestation. Indian J. Plant Prot. 45, 1–7.

Mangrauthia, S.K., Bhogireddy, S., Agarwal, S., Prasanth, V.V., Voleti, S.R., Neelamraju, S., Subrahmanyam, D., 2017a. Genome-wide changes in microRNA expression during short and prolonged heat stress and recovery in contrasting rice cultivars. J. Exp. Bot. 68, 2399–2412.

Mangrauthia, S.K., Malathi, P., Agarwal, S., Ramkumar, G., Krishnaveni, D., Neeraja, C.N., Madhav, M.S., Ladhalakshmi, D., Balachandran, S.M., Viraktamath, B.C., 2012. Genetic variation of coat protein gene among the isolates of Rice tungro spherical virus from tungro-endemic states of the India. Virus Genes 44, 482–487.

Mangrauthia, S.K., Malathi, P., Krishnaveni, D., Reddy, C.S., Viraktamath, B.C., Balachandran, S.M., Neeraja, C.N., Biswal, A.K., 2010. Rapid detection of rice tungro spherical virus by RT-PCR and dot-blot hybridization. J. Mycol. Plant Pathol. 40, 445–449.

Marmey, P., Rojas-Mendoza, A., De Kochko, A., Beachy, R.N., Fauquet, C.M., 2005. Characterization of the protease domain of Rice tungro bacilliform virus responsible for the processing of the capsid protein from the polyprotein. Virol. J. 2, 1–12.

Masuda, T., Fusada, N., Shimada, H., Goto, K., Shibata, D., Kato, T., Tabata, S., Ohta, H., Takamiya, K., 2003. Molecular characterizationof Arabidopsis thaliana T-DNA knockout mutants of POR isozymes (porB and porC) encoding light-dependent protochlorophyllide oxidoreductase. Plant Cell Physiol. Supplement 44, 963–974.

Mathur, S., Dasgupta, I., 2007. Downstream promoter sequence of an Indian isolate of Rice tungro bacilliform virus alters tissue-specific expression in host rice and acts differentially in heterologous system. Plant Mol. Biol. 65, 259–275.

Mauck, K.E., Bosque-Perez, N.A., Eigenbrode, S.D., De Moraes, C.M., Mescher, M.C., 2012. Transmission mechanisms shape pathogen effects on host-vector interactions: evidence from plant viruses. Funct. Ecol. 26, 1162–1175.

McMenemy, L.S., Hartley, S.E., MacFarlane, S.A., Karley, A.J., Shepherd, T., Johnson, S.N., 2012. Raspberry viruses manipulate the behaviour of their insect vectors. Èntomol. Exp. Et. Appl. 144, 56–68.

Mohanty, S.K., Mohanty, S.K., Anjaneyulu, A., Sridhar, R., 1979. Physiology of rice tungro virus disease: involvement of abscisic acid-like substances in susceptible host-virus interactions. Physiol. Plant. 45, 132–136.

Muralidharan, K., Krishnaveni, D., Rajarajeshwari, N.V.L., Prasad, A.S.R., 2003. Tungro epidemic and yield losses in paddy fields in India. Curr. Sci. 85, 1143–1147.

Murray, M., Thompson, W.F., 1980. Rapid isolation of high molecular weight plant DNA. Nucleic Acids Res. 8, 4321–4325.

Rajeswaran, R., Golyaev, V., Seguin, J., Zvereva, A.S., Farinelli, L., Pooggin, M.M., 2014. Interactions of rice tungro bacilliform pararetrovirus and its protein P4 with plant RNA-silencing machinery. Mol. Plant-Microbe Interact. 27, 1370–1378.

Rout, G.R., Sahoo, S., 2015. Role of iron in plant growth and metabolism. Rev. Agric. Sci. 3, 1–24.

Sailaja, B., Anjum, N., Patil, Y.K., Agarwal, S., Malathi, P., Krishnaveni, D., Balachandran, S.M., Viraktamath, B.C., Mangrauthia, S.K., 2013. The complete genome sequence of a south Indian isolate of rice tungro spherical virus reveals evidence of genetic recombination between distinct isolates. Virus Genes 47, 515–523.

Shapiro, L., De Moraes, C.M., Stephenson, A.G., Mescher, M.C., 2012. Pathogen effects on vegetative and floral odours mediate vector attraction and host exposure in a complex pathosystem. Ecol. Lett. 15, 1430–1438.

Shim, J., Torollo, G., Angeles-Shim, R.B., Rogelio, C.C., Cabunagan, R.C., Yeo, U.S., Ha, W.G., 2015. Rice tungro spherical virus resistance into photoperiod-insensitive japonica rice by marker-assisted selection. Breed. Sci. 65, 345–351.

Singh, J., Pal, M., Mishra, M.D., 1990. Effect of rice tungro virus infection on photosynthetic activity in resistant and susceptible rice cultivars. Indian J. Mycol. Plant Pathol. 20, 123–126.

Singh, A.K., Ponnuswamy, R., Donempudi, K., Mangrauthia, S.K., 2015. The differential reaction of rice hybrids to tungro virus by phenotyping and PCR analysis. J. Phytopathol. 164, 177–184.

Sridhar, R., Mohanty, S.K., Anjaneyulu, A., 1978. Physiology of rice tungro virus disease. Increased cytokinin activity in tungro-infected rice cultivars. Physiol. Plant. 43, 363–366.

Srinivasan, R., Alvarez, J.M., Eigenbrode, S.D., Bosque-Perez, N.A., 2006. Influence of hairy nightshade Solanum sarrachoides (Sendtner) and Potato leafroll virus (Luteoviridae, Polerovirus) on the host preference of Myzus periscae (Sulzer) (Homoptera, Aphididae). Environ. Entomol. 35, 546–553.

Subbarao, B.L., Ghosh, A., John, V.T., 1979. Effect of rice tungro virus on chlorophyll and anthocyanin pigments in two rice cultivars. J. Phytopathol. 94, 367–371.

Suzuki, Y., Makino, A., 2012. Availability of Rubisco small subunit up-regulates the transcript levels of large subunit for stoichiometric assembly of its holoenzyme in rice. Plant Physiol. 160, 533–540.

Takagi, S., 1976. Naturally occurring iron-chelating compounds in oat- and rice-root washings. Soil Sci. Plant Nutr. 22, 423–433.

Takahashi, R., Ishimaru, Y., Senoura, T., Shimo, H., Ishikawa, S., Arao, T., Nakanishi, H., Nishizawa, N.K., 2011. The OsNRAMP1 iron transporter is involved in Cd accumulation in rice. J. Exp. Bot. 62, 4843–4850.

Tyagi, H., Rajasubramaniam, S., Rajam, M.V., Dasgupta, I., 2008. RNA-interference in rice against Rice tungro bacilliform virus results in its decreased accumulation in inoculated rice plants. Transgenic Res. 17, 897–904.

Wei, W., Chai, T., Zhang, Y., Han, L., Xu, J., Guan, Z., 2009. The Thlaspi caerulescens NRAMP homologue TcNRAMP3 is capable of divalent cation transport. Mol. Biotechnol. 41, 15–21.

Wu, Z., Zhang, X., He, B., et al., 2007. A chlorophyll-deficient rice mutant with impaired chlorophyllide esterification in chlorophyll biosynthesis. Plant Physiol. 145, 29–40.

Xu, Y., Liu, R., Yan, L., Liu, Z., Jiang, S., Shen, Y., 2012. Light-harvesting chlorophyll a / b -binding proteins are required for stomatal response to abscisic acid in Arabidopsis. J. Exp. Bot. 63, 1095–1106.

Yadav, B.P., Mishra, M.D., 1987. Metabolic changes induced by rice tungro virus in rice cultivars. Indian Phytopathol. 40, 139–148.

Yang, Y., Xu, J., Huang, L., et al., 2016. PGL, encoding chlorophyllide a oxygenase 1, impacts leaf senescence and indirectly affects grain yield and quality in rice. J. Exp. Bot. 67, 1297–1310.